JOURNAL OF AGRICULTURAL AND FOOD CHEMISTRY
ARTICLE

J. Agric. Food Chem. 2009, 57, 4359–4365 4359
DOI:10.1021/jf8035484

Identification of Free Radical Intermediates in Oxidized Wine Using Electron Paramagnetic Resonance Spin Trapping

Ryan J. Elias,[†,§] Mogens L. Andersen,[‡] Leif H. Skibsted,[‡] and Andrew L. Waterhouse*,[†]

[†]Department of Viticulture and Enology, University of California, Davis, California 95616 and [‡]Department of Food Science, University of Copenhagen, DK-1958 Frederiksberg C, Denmark. [§] Present address: Department of Food Science, The Pennsylvania State University, University Park, Pennsylvania 16802.

Free radicals are thought to be key intermediates in the oxidation of wine, but their nature has not been established. Electron paramagnetic resonance spectroscopy was used to detect and identify several free radical species in wine under oxidative conditions with the aid of spin traps. The 1-hydroxylethyl radical was the sole radical species observed when α-(4-pyridyl-1-oxide)-*N*-*tert*-butylnitrone was used as a spin trap in a heated (55 °C), low-sulfite (15 mg L^{-1}) red wine. This radical appears to arise from ethanol oxidation via the hydroxyl radical, and this latter species was confirmed by using a high concentration (1.5 M) of the 5,5-dimethylpyrroline-*N*-oxide spin trap, thus providing the first direct evidence of the Fenton reaction in wine. Hydroxyl radical formation in wine was corroborated by converting hydroxyl radicals to methyl radicals by its reaction with dimethyl sulfoxide. The novel spin trap 5-*tert*-butoxycarbonyl 5-methyl-1-pyrroline *N*-oxide was also used in this study to identify sulfite radicals in wine for the first time. This spin trap has also been shown to trap hydroperoxyl radicals, the generation of which is predicted in wine; however, no evidence of this species was observed.

KEYWORDS: Wine; oxidation; Fenton reaction; EPR; spin trapping; hydroxyl radicals; hydroperoxyl radicals; 1-hydroxyethyl radicals; sulfite radicals; methyl radicals; spin adducts; metal catalysis; iron; copper

INTRODUCTION

The redox chemistry of wine is of great importance with respect to product quality and stability. Many oxidation reactions can lead to deleterious outcomes in wine, such as browning in rosé and white wines (*1*). On the other hand, a certain degree of oxidation is desirable in some cases, particularly in red wines, where limited exposure to oxygen can result in reduced astringency and color stabilization (*2*, *3*). While wine oxidation has been studied for over a century, the modern winemaker has few tools with which to tightly control oxidation to achieve predictable or reproducible results.

It is conceptually convenient to divide the general wine oxidation scheme into two separate steps or reactions. In the first step, dioxygen is brought into the system by reacting with a catechol (e.g., 1,2-hydroquinone). The oxidized polyphenol (e.g., 1,2-benzoquinone) is generated, and oxygen is reduced to hydrogen peroxide (*4*). In a subsequent reaction, hydrogen peroxide is thought to oxidize ethanol to give acetaldehyde (*5*). Recent studies have supported this general mechanism with respect to sequence but have also suggested that redox-active metals may be required to catalyze both reactions and that free radical intermediates are produced during the process (*6*, *7*). Trace levels of transition metals are ubiquitous in wine, with typical concentrations of iron and copper (the most abundant metals in wine) ranging worldwide between 2.8−16 and 0.11−3.6 mg/L, respectively (*8*). In one proposed mechanism, oxygen is converted to a hydroperoxyl radical by a reduced metal (e.g., Fe^{2+}), which then directly oxidizes a catechol to its semiquinone radical (**Scheme 1**). Hydrogen peroxide is formed during this reaction; yet, on the basis of a recent study in our laboratory, it is incapable of directly oxidizing ethanol (*9*). A more likely route for ethanol oxidation at wine pH (∼3.5) is via the hydroxyl radical, which is formed by the iron-catalyzed reduction of hydrogen peroxide (known as the Fenton reaction) (*10*, *11*).

Electron paramagnetic resonance (EPR) spectroscopy is a widely used technique that allows for the direct detection of species with unpaired electrons (e.g., free radicals, transition metals) and can often aid in the determination of the radical's identity. A major limitation to this technique is the inability to directly detect some highly reactive radical species with very short half lives (e.g., superoxide, hydroxyl radicals, sulfur-centered radicals, and alkoxyl radicals) (*12*). This can be overcome through the use of spin traps, which are diamagnetic compounds (often nitrone or nitroso compounds) capable of yielding long-lived radical products upon reaction with free radicals (*12*). EPR spin trapping has been used successfully to elucidate many mechanistic questions in beer oxidation (*13*−*17*); yet, this technique has not been broadly adopted in the study of wine oxidation. In fact, only a limited number of studies have been conducted that address the free radical

*To whom correspondence should be addressed. Fax: 530-752-0382. E-mail: alwaterhouse@ucdavis.edu.

 Published on Web 4/9/2009

Scheme 1. Proposed Metal-Catalyzed Wine Oxidation Mechanism

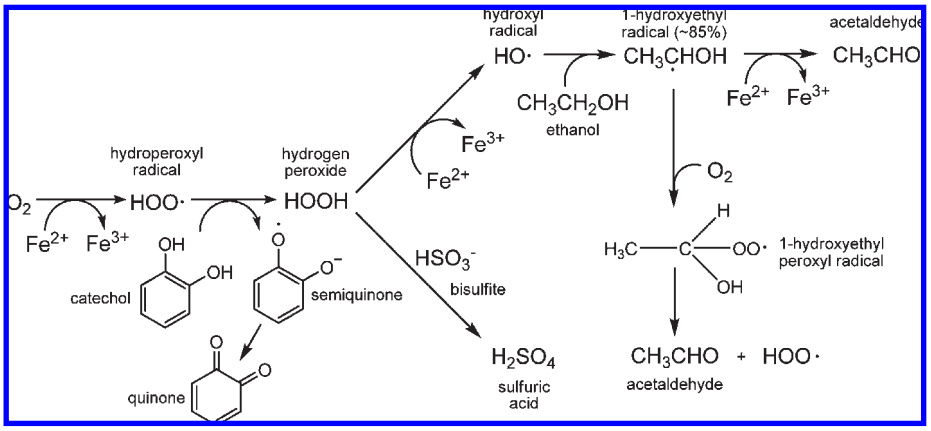

chemistry of wine in general terms (*18*−*20*), many of which involve the detection of persistent phenolic radicals using static EPR (i.e., without the use of spin traps).

The objective of this study was to detect free radical intermediates in wine under oxidative conditions. A variety of spin traps were used to characterize and identify these radicals. It is hoped that the results of this study will help to elucidate key steps in the general mechanism of chemical (i.e., nonenzymatic) wine oxidation.

MATERIALS AND METHODS

Materials. The spin traps 2-methyl-2-nitrosopropane (MNP) (Sigma Aldrich, St. Louis, MO), α-(4-pyridyl-1-oxide)-*N*-*tert*-butylnitrone (POBN) (Sigma), 5,5-dimethylpyrroline-*N*-oxide (DMPO) (Fluka, Buchs, Switzerland), and 5-*tert*-butoxycarbonyl 5-methyl-1-pyrroline *N*-oxide (BMPO) (Alexis Biochemicals, Lausen, Switzerland) were used as received. Iron(II) sulfate heptahydrate (Merck, Darmstadt, Germany) was analytical grade. Copper(II) sulfate pentahydrate, 2,6-dioxopurine (xanthine), (+)-tartaric acid, and hydrogen peroxide (30% w/w solution) were obtained from Sigma Aldrich. 4-Methylcatechol (95%) and ethanol (puriss. pa.) were obtained from Fluka. Potassium metabisulfite was purchased from Bie & Berntsen (Rødovre, Denmark). All other chemicals and solvents were of analytical or high-performance liquid chromatography (HPLC) grade. Water was purified through a Millipore Q-Plus (Millipore Corp., Bedford, MA) purification train. The wine used in this study was Santa Carolina Cabernet Sauvignon 2006, D.O. Valle del Rapel (Chile), containing 13.5% (v/v) ethanol and a total (free and bound) sulfur dioxide concentration of 88 mg L^{-1}. The total sulfur dioxide was measured using a kit adapted from Rebelein's method (C. Schliessmann Kellerei-Chemie GmbH). A model wine consisting of 12% (v/v) ethanol and (+)-tartaric acid (8.0 g L^{-1}), adjusted to pH 3.6 with 1 N NaOH, with or without 4-methylcatechol (1.2 g L^{-1}), was prepared as described previously (*6*).

Sulfur Dioxide Removal. The final sulfur dioxide concentration of Cabernet Sauvignon (CabS) was adjusted downward by the slow, stepwise addition of hydrogen peroxide (3% v/v). Briefly, three additions of H_2O_2 (16 μL) were added to the CabS (50 mL, containing 88 mg L^{-1} total SO_2) at 20 min intervals. The wine was treated in a 250 mL glass media bottle, was mechanically agitated with a magnetic stir bar under a nitrogen gas headspace, and was protected from light. The treated wine was blanketed with nitrogen gas, capped, and was held at room temperature for 4 h before SO_2 analysis was performed. The final total SO_2 was 15 mg L^{-1}.

Metal Analysis. The concentrations of endogenous transition metals in the wine were measured by inductively coupled plasma mass spectrometry (ICP-MS). Wine (25 mL) was concentrated to dryness using rotational vacuum concentration. The precipitate was resuspended in 250 μL of ultrapure HNO_3 (70%). Acid digestion and ICP-MS analysis of Fe, Cu, and Mn were performed as previously described (*21*).

ESR Spin Trapping. The POBN, DMPO, and BMPO spin traps were dissolved directly into wine or model wine samples (1−2 mL). The final concentrations of POBN, BMPO, and DMPO were 15 mM, 25 mM, and 1.5 M, respectively. MNP (14.8 mg) was either directly dissolved in the sample or dissolved in dimethyl sulfoxide (DMSO; 0.71 mL) and mixed by vortex prior to addition to the sample to give a final MNP concentration of 17 mM. The samples were kept in capped glass culture tubes with a headspace volume of ~8 mL air at either room temperature or at 55 °C in a heated water bath. All wine samples were protected from light during the study. In some experiments, Fe(II) and/or Cu(II) were added (10 μL) from freshly prepared stock solutions in deoxygenated water. Hydrogen peroxide was added (10 μL) in some cases from a working solution (30 mM in water) prepared daily from a stock solution (3.0 M). Samples (50 μL) were loaded into 50 μL micropipettes (Brand GmbH, Wertheim, Germany), and the EPR spectra were recorded on a Miniscope MS 200 X-band spectrometer (Magnettech, Berlin, Germany) at room temperature. The EPR microwave power was set to 10 mW, the modulation frequency was 1000 mG, and a sweep time of 60 s was used. A sweep width of 68 G was used for experiments with POBN and DMPO, and 98 G was used for experiments with MNP and BMPO. The receiver gain was set to either 90 or 900, depending on the experiment and abundance of spin adducts. EPR calibration was performed using 2,2,6,6-tetramethylpiperidine-1-oxyl (2 μM). Simulation and fitting of the EPR spectra were performed using the PEST WinSIM program (*22*).

RESULTS AND DISCUSSION

Formation of 1-Hydroxyethyl Radicals in Wine. The spin trap POBN (**Figure 1**) gives spin adducts with long half-lives, allowing for the detection of radical species formed over the course of several days, and often at elevated temperatures. POBN (15 mM) was added to reduced sulfite CabS ($[SO_2]_0$ = 15 mg L^{-1}) and incubated at 55 °C. The wine's sulfite concentration was lowered to reduce the lag phase that precedes ethanol oxidation (*16*). The presence of spin adducts giving rise to a six-line spectrum was clearly observable after 2 h of incubation at 55 °C (**Figure 2**), indicating the presence of free radical intermediates in the wine. The concentration of POBN spin adducts increased over the course of 44 h, as was evidenced by comparing the peak-to-peak amplitudes of the EPR signals. The hyperfine coupling constants of the observed spectrum (a_N = 15.4 G, a_H = 2.6 G) were nearly identical to the values for the POBN spin adducts formed from the 1-hydroxyethyl radical

(MeCH•OH) (*12*). When a Fenton system ([H_2O_2] = 0.3 mM; [Fe^{2+}] = 50 μM) was established in the same low-sulfite wine, the same six-line spectrum (a_N = 15.4 G, a_H = 2.5 G) corresponding to the 1-hydroxylethyl radical was observed (**Figure 3**). The same characteristic spectrum with identical coupling constants was observed when H_2O_2 and Fe^{2+} were added to a model wine system in both the presence and the absence of 4-methylcatechol (data not shown). The experimental ESR spectra could all be perfectly simulated by assuming that only a single spin adduct contributed to the ESR spectra. The 1-hydroxyethyl radical is proposed to be the major species resulting from the hydroxyl radical-mediated oxidation of ethanol. Hydrogen abstraction is preferred at ethanol's C-1 carbon and results in the 1-hydroxyethyl radical in high yield (~85%) (*23*). Under aerobic conditions, 1-hydroxyethyl radicals are thought to react at diffusion-controlled rates with oxygen, eventually degrading to acetaldehyde. The 2-hydroxyethyl radical is also formed during ethanol oxidation (reaction at the C-2 carbon) but is considered a minor species.

These data suggest that, in quantitative terms, the 1-hydroxyethyl radical is the major radical species in wine. This is consistent with the proposed oxidation scheme of beer (*13*), where accelerated conditions were also shown to produce the same radicals as at room temperature (*17*). As expected based on the high reactivity of the hydroxyl radical, the formation of the 1-hydroxyethyl radical is not prevented or impeded by the large excess of wine's endogenous polyphenols, which are widely accepted antioxidants. This is because the radical will attack the first species it encounters, which is ethanol due to its greater abundance.

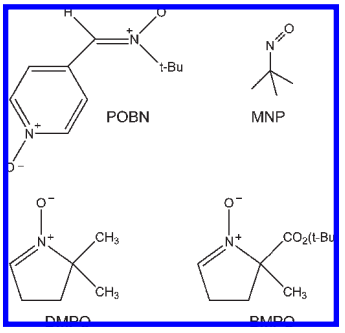

Figure 1. Spin traps used in this study: POBN, MNP, DMPO, and BMPO.

Evidence of Hydroxyl Radical Formation in Wine. The direct detection of hydroxyl radicals (•OH) in a wine system is complicated by the abundance of ethanol, which itself is a substrate for hydroxyl radicals and thus competes with the spin trap (*13*). The concentration of ethanol in wine varies by style and region of origin, but levels are at molar concentrations (~2 M). It is therefore necessary to establish a large concentration of the spin trap to intercept a sufficient quantity of hydroxyl radicals required for analysis. When hydrogen peroxide and iron ([H_2O_2] = 0.3 mM; [Fe^{2+}] = 50 μM) were added to wine containing the low-sulfite CabS in the presence of a high concentration of the DMPO spin trap (1.5 M), two spectra corresponding to two distinct radical species were observed (**Figure 4**). The first spectrum was a triplet of doublets with hyperfine coupling constants (a_N = 15.6 G, a_H = 22.5 G) indicative of the 1-hydroxyethyl radical, as was observed using the POBN spin trap. However, a second spectrum was also observed, apparently due to the DMPO/•OH adduct (coupling constants a_N = 14.7 G, a_H = 14.0 G). On the basis of the digital simulation of the ESR spectrum, the relative abundances of the DMPO/MeCH•OH and DMPO/•OH adducts were 60 and 40%, respectively. The DMPO/•OH signal disappeared when the concentration of DMPO was reduced (data not shown).

After the feasibility of trapping the hydroxyl radical in a real wine system under Fenton conditions was established, the generation of hydroxyl radicals was investigated in low-sulfite CabS without added hydrogen peroxide or metal. The concentrations of endogenous iron, copper, and manganese were 11.2, 0.72, and 27.2 μM, respectively. Because of the relatively low stability of the DMPO/•OH adducts, the wine was allowed to oxidize at room temperature in the absence of light for 2 h. No DMPO/•OH adducts could be observed under these conditions; however, adducts were observed when iron ($[Fe(II)]_{added}$ = 89.6 μM; $[Fe]_{total}$ = 100.8 μM) and copper ($[Cu(II)]_{added}$ = 6.3 μM; $[Cu]_{total}$ = 7.0 μM) were added to

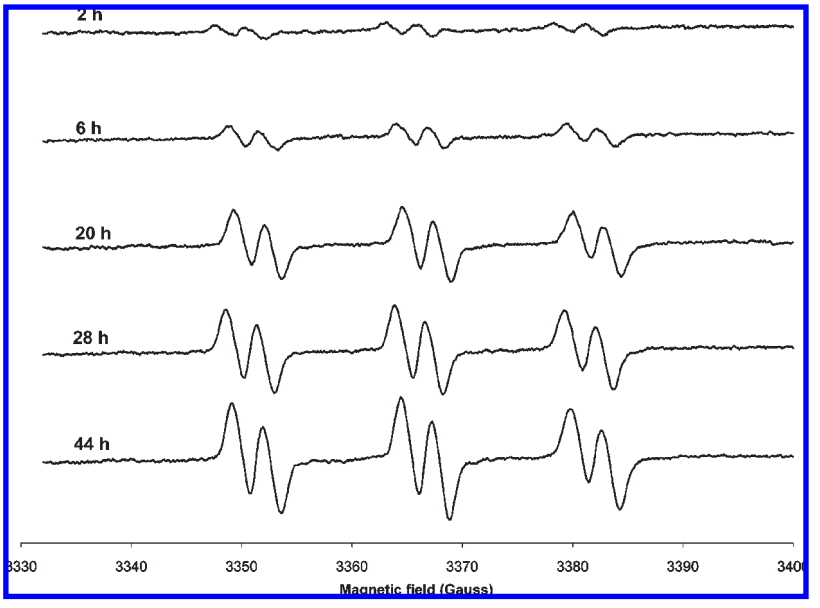

Figure 2. EPR spectrum of POBN/1-hydroxyethyl radical (MeCH•OH) spin adducts in low sulfite (15 mg L^{-1} SO_2), heated (55 °C) CabS taken after 2, 6, 20, 28, and 44 h.

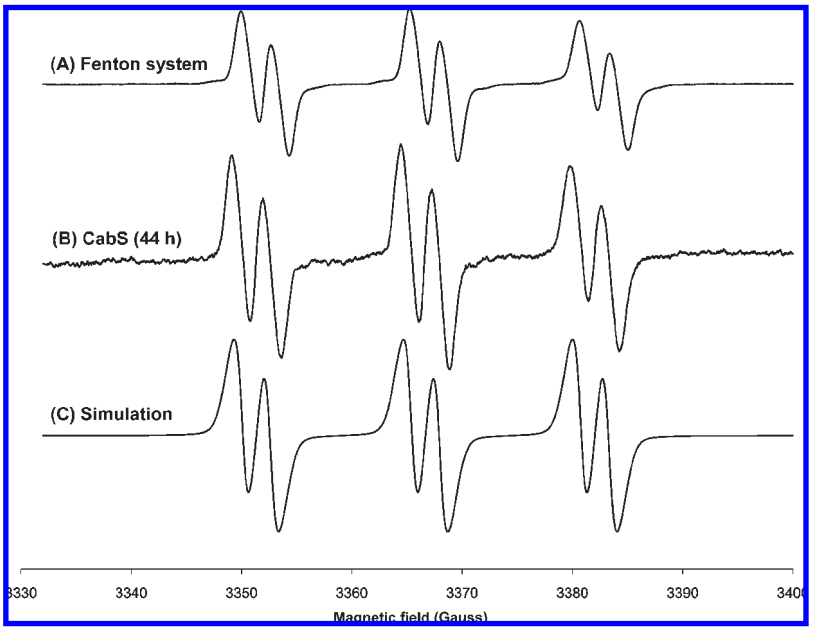

Figure 3. Experimental spin patterns of POBN/1-hydroxyethyl radical (MeCH$^{\bullet}$OH) spin adducts in low sulfite (15 mg L^{-1} SO_2) CabS after addition of H_2O_2 (0.3 mM) and Fe^{2+} (50 μM) (**A**). The second (**B**) and third (**C**) sets of spectra show the experimental and simulated (respectively) spin patterns of the same wine that has been heated (55 °C; 44 h) without added H_2O_2 and Fe^{2+}.

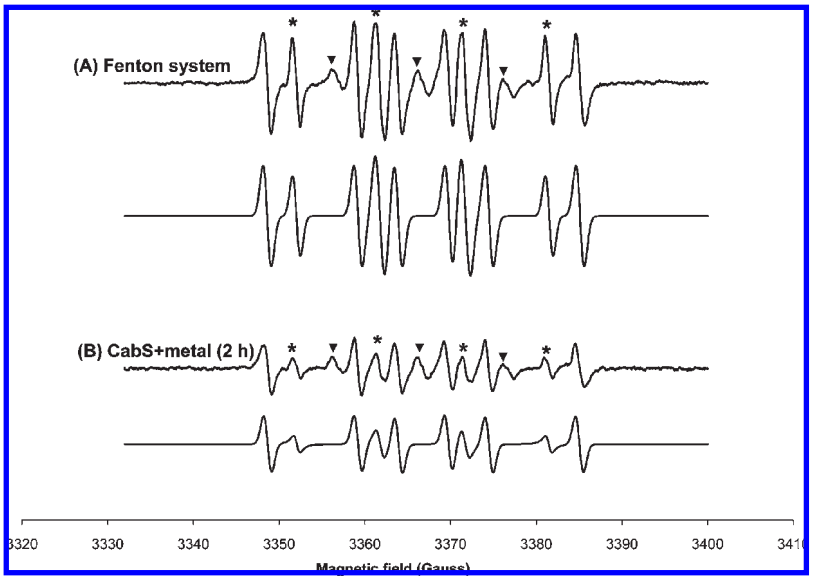

Figure 4. EPR spectra (upper trace = experimental; lower trace = simulated) of DMPO spin adducts in low sulfite (15 mg L^{-1} SO_2) CabS after addition of H_2O_2 (0.3 mM) and Fe^{2+} (50 μM) (**A**). The second set of spectra (upper trace = experimental; lower trace = simulated) are DMPO spin adducts formed in CabS (room temperature; 2 h) with added Fe^{2+} (**B**). DMPO/$^{\bullet}$OH spin adducts are denoted (*). Unmarked peaks are attributed to DMPO/MeCH$^{\bullet}$OH adducts. Unassigned spin adducts are denoted (▼).

the low-sulfite wine (**Figure 4**). The final, total concentrations of these added metals ($[Fe]_{total}$ = 5.6 mg L^{-1}; $[Cu]_{total}$ = 0.45 mg L^{-1}) were still within the range of iron and copper levels found in wines worldwide, as the average concentration of iron in wines globally is ~5.5 mg L^{-1}, and copper concentrations are reported to range from 0.1 to 0.3 mg L^{-1}(*6*).

The spin trap MNP was also used to confirm the presence of hydroxyl radicals in wine. The hyperfine couplings of MNP's spin adducts are extremely sensitive to the trapped species' structure because the spin trap's nitroxyl moiety is bonded directly to the radical (*13*). As such, a Fenton system (described above) was established in the low-sulfite wine with the aim of trapping hydroxyl radicals; however, the MNP/$^{\bullet}$OH adduct is not stable and could not be discerned from the EPR spectrum. Crystalline MNP exists as a dimer; yet, the active spin trapping form is the MNP monomer, which is formed in solution. Approximately 12 h was required (constant stirring under dark glass; room temperature) to completely dissolve the solid MNP dimer in either the wine or the model wine systems, but by this time, the spin trap had apparently degraded considerably, resulting in excessive background noise. Thus, an alternative method was adapted in which MNP was dissolved directly into DMSO (complete solubility within ~1 min after vortex mixing at room temperature). The spin trap solution was added directly to the wine sample (17 mM MNP; 1 M DMSO), at which point the Fenton reaction was initiated

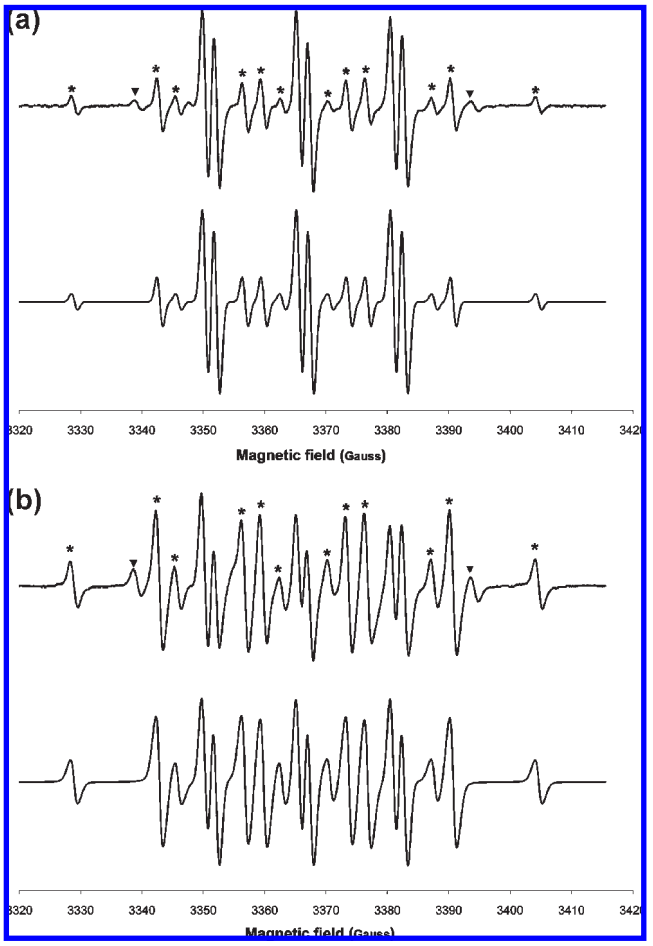

Figure 5. EPR spectra of MNP spin adducts in low sulfite (15 mg L^{-1} SO_2) CabS with DMSO (1 M) (**A**) and in ethanol solution (2 M) with DMSO (1 M) (**B**). Upper and lower traces are experimental and simulated spectra, respectively. MNP/$^{\bullet}CH_3$ spin adducts are denoted (*). Unmarked peaks are attributed to MNP/MeCH$^{\bullet}$OH adducts. Unassigned spin adducts are denoted (▼).

Scheme 2. Spin Trapping of Methyl Radicals ($^{\bullet}CH_3$) Resulting from the Oxidation of DMSO by a Hydroxyl Radical ($^{\bullet}$OH)

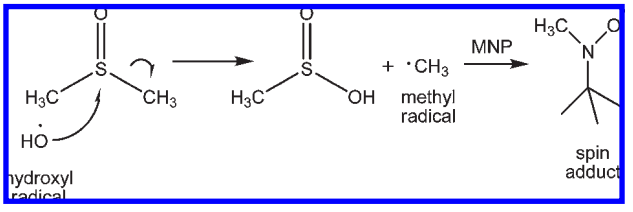

and EPR analysis was performed. The oxidation of DMSO by the hydroxyl radical yields a methyl radical that can subsequently be trapped by MNP (**Scheme 2**). A spectrum characteristic of the MNP/$^{\bullet}CH_3$ spin adduct was observed in the CabS + DMSO (1 M) system (**Figure 5a**), and had hyperfine coupling constants (a_N = 17.1 G, a_H = 14.0 G) that were consistent with those reported for MNP/$^{\bullet}CH_3$ radicals (*12*). The observation of methyl radicals provides indirect evidence of the hydroxyl radical in this system and circumvents the many artifacts associated with DMPO/$^{\bullet}$OH formation (*24*). Included in the CabS + DMSO (1 M) EPR spectrum were spin adducts that gave identical coupling constants (a_N = 15.5 G, a_H = 1.8 G) to those reported for MNP/MeCH$^{\bullet}$OH radicals (*12*). In fact, the 1-hydroxyethyl radical proved to be the most quantitatively important

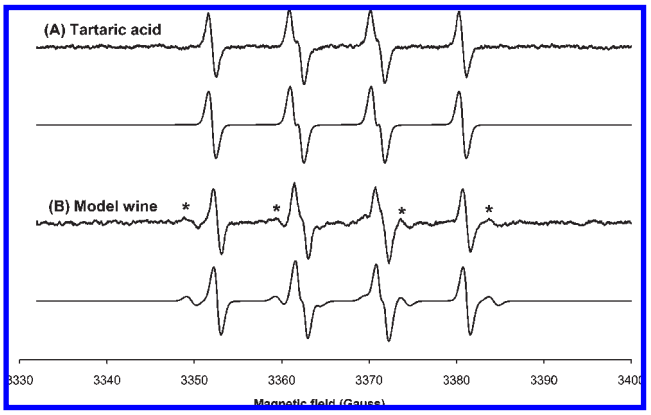

Figure 6. EPR spectra of BMPO spin adducts in tartaric acid solution (53.3 mM, pH 3.6 with 1 N NaOH) (**A**) and model wine (**B**). Upper and lower traces are experimental and simulated spectra, respectively. BMPO/ MeCH$^{\bullet}$OH spin adducts are denoted (*).

radical in this system, accounting for 77% of the total observed spin adducts, again supporting the observation above that the 1-hydroxyethyl radical is the most abundant radical in oxidized wine. EPR spectra with similar splitting patterns were observed when hydrogen peroxide and iron were added to a simple ethanol solution (2 M) containing MNP and DMSO (**Figure 5b**).

Spin Trapping of Sulfite Radicals with BMPO. Given the large concentration of sulfite in wine, as well as the presence of endogenous trace metals, the formation of sulfite radicals is possible (*6*), yet has not been the focus of considerable study. Low levels of sulfite are produced in wine during primary fermentation; however, the majority of sulfite found in commercial wines is added and may be present in wine at concentrations up to (or exceeding) 100 mg L^{-1} (1.56 mM). The metal-catalyzed autoxidation of sulfite to sulfite radicals ($SO_3^{-\bullet}$) has been established under acidic conditions (*25*, *26*). If this species is in fact generated under wine conditions, its fate has yet to be elucidated, although it may participate in subsequent reactions with oxygen (if present) and bisulfite to yield more potent sulfur oxide derived radicals (e.g., $SO_5^{-\bullet}$ and $SO_4^{-\bullet}$) (*6*, *26*).

The production of sulfite radicals under wine conditions was investigated using the novel spin trap, BMPO (**Figure 1**). This nitrone spin trap has been shown to give sulfite radical spin adducts with relatively long half-lives (*27*, *28*). Because of the lack of published hyperfine coupling constants for these BMPO adducts at the time, several experiments were performed in model systems as the basis for assigning observed EPR signals to spin adducts. For example, a four line spectrum (a_N = 13.6 G, a_H = 14.8 G) was the only signal observed after 18 h (room temperature) when SO_2 (3.13 mM) was added to an EPR-silent solution of tartaric acid (53.3 mM, pH 3.6 with 1 N NaOH) containing Fe(II) (89.6 μM), Cu(II) (6.3 μM), and BMPO (25 mM) (**Figure 6**) and was thus attributed to the BMPO/$SO_3^{\bullet}$ species. The faint appearance of a second spin adduct (a_N = 14.9 G, a_H = 21.0 G), presumably BMPO/MeCH$^{\bullet}$OH, was observed when ethanol (2 M) was added to the same system (**Figure 6**). These coupling constants are somewhat similar to those values reported for the DMPO/$SO_3^{\bullet}$ (a_N = 14.4 G, a_H = 15.9 G) and DMPO/ MeCH$^{\bullet}$OH (a_N = 15.7 G, a_H = 22.4 G) adducts (*12*), despite the fact that BMPO differs from DMPO with respect to its *t*-butyl moiety.

In this experiment, the trapping of sulfite radicals was attempted in a real wine system. When both Fe(II) (89.6 μM)

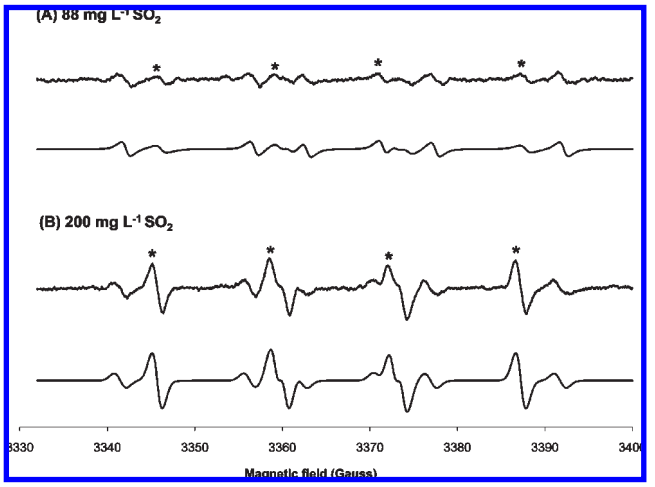

Figure 7. EPR spectra of BMPO spin adducts in untreated (88 mg L^{-1} SO_2) (**A**) and high sulfite (200 mg L^{-1} SO_2) (**B**) CabS. Upper and lower traces are experimental and simulated spectra, respectively. BMPO/$SO_3^{-\bullet}$ spin adducts are denoted (*).

Scheme 3. Proposed Mechanism Showing the Reactivity of Various Sulfur Oxide Derived Radical Species with a Spin Trap, Catechol, or Ethanol

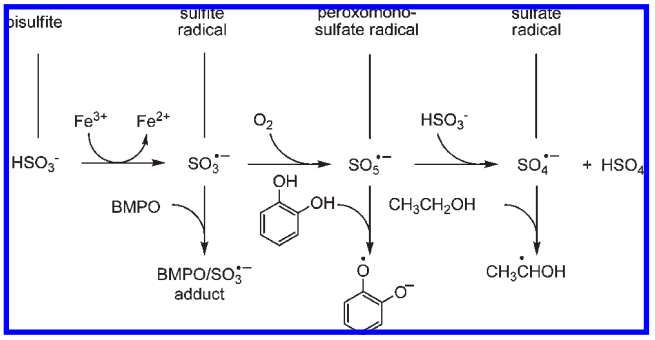

and Cu(II) (6.3 μM) were added to CabS ($[SO_2]_{total}$ = 88 mg L^{-1}, 1.38 mM) in the absence of light, two distinct BMPO spin adducts were observed in the EPR spectrum after 18 h (room temperature), which were assigned to the BMPO/MeCH$^{\bullet}$OH (a_N = 14.7 G, a_H = 20.7 G) and BMPO/$SO_3^{\bullet}$ (a_N = 13.4 G, a_H = 14.6 G) adducts (**Figure 7**). The intensity of the apparent BMPO/$SO_3^{-\bullet}$ signals was found to increase markedly when an additional 112 mg L^{-1} SO_2 ($[SO_2]_{total}$ = 200 mg L^{-1}, 3.13 mM) was added to the same wine after 18 h (incubation at room temperature). However, no increase in BMPO/MeCH$^{\bullet}$OH intensity was observed in the SO_2 concentration treatment, suggesting that the sulfite radicals formed were not able to oxidize ethanol to any significant degree. The fate of the sulfite radical ($SO_3^{-\bullet}$) in this system is proposed in **Scheme 3**, wherein $SO_3^{-\bullet}$ reacts with O_2 to yield a peroxomonosulfate radical ($SO_5^{-\bullet}$) (*26*). In the presence of BMPO, it appears the spin trap competes with oxygen for the $SO_3^{-\bullet}$ radical, and the resulting spin adduct becomes evident in the EPR spectrum. While it appears the $SO_3^{-\bullet}$ radical cannot directly oxidize catechols, its peroxomonosulfate form is a considerably more potent oxidant (E = 1.17 V for the $SO_5^{-\bullet}/HSO_5^-$ couple at pH 3.5) and is capable of oxidizing polyphenols under wine conditions (*6*, *29*). In the absence of a good hydrogen donor, $SO_5^{-\bullet}$ reacts with bisulfite (HSO_3^-) to yield the highly oxidizing sulfate radical ($SO_4^{-\bullet}$) species, which itself is capable of oxidizing ethanol; however, in a wine system, this route for

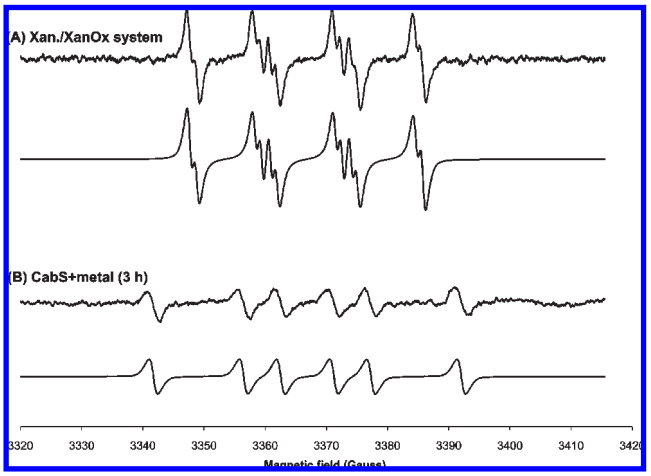

Figure 8. EPR spectra of BMPO/$^{\bullet}$OOH spin adducts generated in a xanthine/xanthine oxidase system (**A**) and BMPO/ MeCH$^{\bullet}$OH spin adducts formed in low sulfite (15 mg L^{-1} SO_2) CabS (room temperature; 3 h) (**B**). Upper and lower traces are experimental and simulated spectra, respectively.

1-hydroxyethyl radical production is essentially cut off by polyphenol scavenging of $SO_5^{-\bullet}$ radicals. Such an observation is consistent with that of Danilewicz, who showed that the sulfite radical-mediated oxidation of ethanol in a simple model wine was all but completely shut down when 4-methylcatechol was added (*6*).

Lack of Evidence of Hydroperoxyl Radical Formation in Wine. The formation of hydroperoxyl radicals resulting from the metal-catalyzed reduction of dioxygen is predicted under wine conditions (**Scheme 1**) (*10*, *11*); yet, no conclusive evidence of this intermediate has been reported to date. BMPO is capable of reacting with hydroperoxyl radicals to yield stable spin adducts with good signal-to-noise ratios (*27*, *28*), thus making it an ideal spin trap for studying this radical in wine. The viability of detecting BMPO/HOO$^{\bullet}$ spin adducts was first determined by using a xanthine/xanthine oxidase system to produce hydroperoxyl radicals, as described previously (*28*). The observed BMPO/HOO$^{\bullet}$ spin adducts (a_N = 13.3 G, a_H = 12.1 G) gave a characteristic EPR spectrum that was consistent with previous reports, and similar coupling constants to those reported in the literature were observed (**Figure 8**) (*28*). No BMPO/HOO$^{\bullet}$ spin adducts were observed in a real wine system (low SO_2 CabS) with added metals ($[Fe(II)]_{added}$ = 89.6 μM; $[Cu(II)]_{added}$ = 6.3 μM) after 3 h (incubated at room temperature). However, a six line spectrum corresponding to the BMPO/ MeCH$^{\bullet}$OH spin adduct (a_N = 14.9 G, a_H = 21.0 G) was observed in the same wine after 3 h (**Figure 8**). It should be noted that the hydroperoxyl radical adduct would be the least stable of the expected adducts, and perhaps, it is hard to detect in the presence of these other more stable products.

These data may suggest that the generation of hydrogen peroxide in wine does not occur via a hydroperoxyl radical intermediate. Oxygen may react directly with a metal−catechol complex to yield hydrogen peroxide (and quinone), thereby bypassing the formation of hydroperoxyl radicals. Such a mechanism has been proposed at physiological pH (*30*−*32*) but is not predicted under wine conditions due to iron's ability to directly reduce oxygen by a one-electron addition. Alternatively, the half-life of the BMPO/HOO$^{\bullet}$ spin adducts may be extremely short under wine conditions and may be swiftly degraded to EPR-silent species.

It is also possible that the reaction between the hydroperoxyl radicals and the wine's endogenous polyphenols is exceedingly fast, effectively outcompeting the BMPO−hydroperoxyl radical reaction. However, if dioxygen is reduced solely by the sulfite radical pathway, it is not clear how hydrogen peroxide could arise.

In conclusion, these data provide evidence that wine oxidation is governed by radical-mediated processes and that several key steps are catalyzed by transition metals. The reaction of ethanol with the Fenton-generated hydroxyl radical is all but proven by the consistent appearance of hydroxyethyl radicals as the major radical species in wine. The necessary use of a nearly equimolar concentration of DMPO in the presence of ethanol to trap the hydroxyl radical also confirms the futility of trace antioxidants in scavenging that hydroxyl radical. Thus, better control of this wine oxidation step must intervene prior to the Fenton reaction. On the other hand, the observation of sulfite radicals shows that more attention is needed to explain the dioxygen reduction steps and the formation of hydrogen peroxide.

LITERATURE CITED

(1) Singleton, V. L.; Trousdale, E.; Zaya, J. Oxidation of wines. 1. Young white wines periodically exposed to air. *Am. J. Enol. Vitic*. **1979**, *30*, 49–54.

(2) Atanasova, V.; Fulcrand, H.; Cheynier, W.; Moutounet, M. Effect of oxygenation on polyphenol changes occurring in the course of wine-making. *Anal. Chim. Acta* **2002**, *458*, 15–27.

(3) Castellari, M.; Arfelli, G.; Riponi, C.; Amati, A. Evolution of phenolic compounds in red winemaking as affected by must oxygenation. *Am. J. Enol. Vitic*. **1998**, *49*, 91–94.

(4) Cilliers, J. J. L.; Singleton, V. L. Nonenzymic autoxidative reactions of caffeic acid in wine. *Am. J. Enol. Vitic*. **1990**, *41*, 84–86.

(5) Wildenradt, H. L.; Singleton, V. L. Production of aldehydes as a result of oxidation of polyphenolic compounds and its relation to wine aging. *Am. J. Enol. Vitic*. **1974**, *25*, 119–126.

(6) Danilewicz, J. C. Interaction of sulfur dioxide, polyphenols, and oxygen in a wine-model system: Central role of iron and copper. *Am. J. Enol. Vitic*. **2007**, *58*, 53–60.

(7) Danilewicz, J. C.; Seccombe, J. T.; Whelan, J. Mechanism of interaction of polyphenols, oxygen, and sulfur dioxide in model wine and wine. *Am. J. Enol. Vitic*. **2008**, *59*, 128–136.

(8) Ough, C. S.; Amerine, M. A. *Methods for Analysis of Musts and Wines*, 2nd ed.; J. Wiley: New York, 1988; p x, 377.

(9) Laurie, V. F.; Waterhouse, A. L. Oxidation of glycerol in the presence of hydrogen peroxide and iron in model solutions and wine. Potential effects on wine color. *J. Agric. Food Chem*. **2006**, *54*, 4668–4673.

(10) Waterhouse, A. L.; Laurie, V. F. Oxidation of wine phenolics: A critical evaluation and hypotheses. *Am. J. Enol. Vitic*. **2006**, *57*, 306–313.

(11) Danilewicz, J. C. Review of reaction mechanisms of oxygen and proposed intermediate reduction products in wine: Central role of iron and copper. *Am. J. Enol. Vitic*. **2003**, *54*, 73–85.

(12) Buettner, G. R. Spin trapping: ESR parameters of spin adducts. *Free Radical Biol. Med*. **1987**, *3*, 259–303.

(13) Andersen, M. L.; Skibsted, L. H. Electron spin resonance spin trapping identification of radicals formed during aerobic forced aging of beer. *J. Agric. Food Chem*. **1998**, *46*, 1272–1275.

(14) Frederiksen, A. M.; Festersen, R. M.; Andersen, M. L. Oxidative reactions during early stages of beer brewing studied by electron spin resonance and spin trapping. *J. Agric. Food Chem*. **2008**, *56*, 8514–20.

(15) Uchida, M.; Ono, M. Determination of hydrogen peroxide in beer and its role in beer oxidation. *J. Am. Soc. Brew. Chem*. **1999**, *57*, 145–150.

(16) Uchida, M.; Ono, M. Improvement for oxidative flavor stability of beer—Role of OH-radical in beer oxidation. *J. Am. Soc. Brew. Chem*. **1996**, *54*, 198–204.

(17) Uchida, M.; Suga, S.; Ono, M. Improvement for oxidative flavor stability of beer—Rapid prediction method for beer flavor stability by electron spin resonance spectroscopy. *J. Am. Soc. Brew. Chem*. **1996**, *54*, 205–211.

(18) Glidewell, S. M.; Deighton, N.; Goodman, B. A.; Troup, G. J.; Hutton, D. R.; Hewitt, D. G.; Hunter, C. R. Free radical scavenging abilities of beverages. *Int. J. Food Sci. Technol*. **1995**, *30*, 535–537.

(19) Troup, G. J.; Hunter, C. R. EPR free radicals, wine, and the industry—Some achievements. *Alcohol Wine Health Dis*. **2002**, *957*, 345–347.

(20) Troup, G. J.; Hutton, D. R.; Hewitt, D. G.; Hunter, C. R. Free-radicals in red wine, but not in white. *Free Radical Res*. **1994**, *20*, 63–68.

(21) Persson, D. P.; Hansen, T. H.; Holm, P. E.; Schjoerring J. K.; Hansen, H. C. B.; Nielsen, J.; Cakmak, I.; Husted, S. Multi-elemental speciation analysis of barley genotypes differing in tolerance to cadmium toxicity using SEC-ICP-MS and ESI-TOF-MS. *J. Anal. At. Spectrom*. **2006**, *21*, 996–1005.

(22) Duling, D. R. Simulation of multiple isotropic spin-trap EPR-spectra. *J. Magn. Reson. Ser. B* **1994**, *104*, 105–110.

(23) Asmus, K. D.; Mockel, H.; Henglein, A. Pulse radiolytic study of site of oh radical attack on aliphatic alcohols in aqueous-solution. *J. Phys. Chem*. **1973**, *77*, 1218–1221.

(24) Mason, R. P.; Kadiiska, M. B. Biomedical EPR, part A: Free radicals, metals, medicine, and physiology. *Biological Magnetic Resonance*; Springer US: New York, 2004; Vol. *23*, pp 93−109.

(25) Brandt, C.; Fabian, I.; Vaneldik, R. Kinetics and mechanism of the iron(III)-catalyzed autoxidation of sulfur(IV) oxides in aqueous-solution—Evidence for the redox cycling of iron in the presence of oxygen and modeling of the overall reaction-mechanism. *Inorg. Chem*. **1994**, *33*, 687–701.

(26) Brandt, C.; Vaneldik, R. Transition-metal-catalyzed oxidation of sulfur(IV) oxides—Atmospheric-relevant processes and mechanisms. *Chem. Rev*. **1995**, *95*, 119–190.

(27) Khan, N.; Wilmot, C. M.; Rosen, G. M.; Demidenko, E.; Sun, J.; Joseph, J.; O'Hara, J.; Kalyanaraman, B.; Swartz, H. M. Spin traps: In vitro toxicity and stability of radical adducts. *Free Radical Biol. Med*. **2003**, *34*, 1473–81.

(28) Zhao, H.; Joseph, J.; Zhang, H.; Karoui, H.; Kalyanaraman, B. Synthesis and biochemical applications of a solid cyclic nitrone spin trap: A relatively superior trap for detecting superoxide anions and glutathiyl radicals. *Free Radical Biol. Med*. **2001**, *31*, 599–606.

(29) Das, T. N.; Huie, R. E.; Neta, P. Reduction potentials of $SO_3^{\bullet-}$, $SO_5^{\bullet-}$, and $S_4O_6^{\bullet 3-}$ radicals in aqueous solution. *J. Phys. Chem. A* **1999**, *103*, 3581–3588.

(30) Bandy, B.; Davison, A. J. Interactions between metals, ligands, and oxygen in the autoxidation of 6-hydroxydopamine—Mechanisms by which metal chelation enhances inhibition by superoxide-dismutase. *Arch. Biochem. Biophys*. **1987**, *259*, 305–315.

(31) Gee, P.; Davison, A. J. 6-Hydroxydopamine does not reduce molecular-oxygen directly, but requires a coreductant. *Arch. Biochem. Biophys*. **1984**, *231*, 164–168.

(32) Gee, P.; Davison, A. J. Autoxidation of 6-hydroxydopamine involves a ternary reductant-metal-oxygen complex. *Ircs Med. Sci.-Biochem*. **1984**, *12*, 127–127.

Received for Review November 13, 2008. Accepted February 24, 2009. Revised manuscript received February 23, 2009.